

On the Use of Gaussian Approximation in Analyzing the Performance of Optical Receivers

Volume 6, Number 1, February 2014

G. El-Howayek, Student Member, IEEE

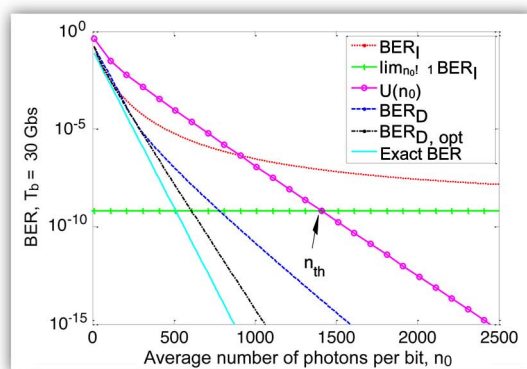
C. Zhang

Y. Li

J. S. Ng, Member, IEEE

J. P. R. David, Fellow, IEEE

M. M. Hayat, Fellow, IEEE



$$n_{th} \equiv -\frac{1}{c_2} \ln \left[\sqrt{\pi} \operatorname{erfc} \left(\frac{\beta_{\mu} \sqrt{1 - e^{-2\kappa\lambda}}}{\sqrt{2} e^{-\kappa\lambda} \alpha_{\mu}} \right) \right]$$

$$\lim_{n_0 \rightarrow \infty} \operatorname{BER}_I = \frac{1}{2} \operatorname{erfc} \left(\frac{\beta_{\mu} \sqrt{1 - e^{-2\kappa\lambda}}}{\sqrt{2} e^{-\kappa\lambda} \alpha_{\mu}} \right)$$

$$\operatorname{BER}_D < \frac{1}{4\sqrt{\pi}} \left(\frac{e^{-c_1^2 n_0}}{c_1 \sqrt{n_0}} + \frac{e^{-c_2^2 n_0}}{c_2 \sqrt{n_0}} \right)$$

DOI: 10.1109/JPHOT.2014.2302792

1943-0655 © 2014 IEEE

On the Use of Gaussian Approximation in Analyzing the Performance of Optical Receivers

G. El-Howayek,¹ *Student Member, IEEE*, C. Zhang,² Y. Li,³
J. S. Ng,⁴ *Member, IEEE*, J. P. R. David,⁴ *Fellow, IEEE*, and
M. M. Hayat,¹ *Fellow, IEEE*

¹Center of High Technology Materials and Department of Electrical and Computer Engineering, University of New Mexico, Albuquerque, NM 87131-0001 USA

²Department of Electrical Engineering and Computer Science, University of Michigan, Ann Arbor, MI 48109 USA

³Department of Electrical and Computer Engineering, University of Illinois at Urbana-Champaign, Champaign, IL 61820 USA

⁴Department of Electronic and Electrical Engineering, University of Sheffield, Sheffield, S1 3JD U.K.

DOI: 10.1109/JPHOT.2014.2302792

1943-0655 © 2014 IEEE. Translations and content mining are permitted for academic research only. Personal use is also permitted, but republication/redistribution requires IEEE permission.

See http://www.ieee.org/publications_standards/publications/rights/index.html for more information.

Manuscript received December 31, 2013; revised January 14, 2014; accepted January 15, 2014. Date of publication January 27, 2014; date of current version February 11, 2014. This work was supported in part by the National Science Foundation under Award ECS-0601645 and in part by the University of New Mexico's Science and Technology Corporation (STC.UNM). Jo S. Ng would like to acknowledge funding from the Royal Society for her University Research Fellowship. Corresponding author: G. El-Howayek (e-mail: ghowayek@ece.unm.edu).

Abstract: The analytical calculation of the bit error rate (BER) of digital optical receivers that employ avalanche photodiodes (APDs) is challenging due to 1) the stochastic nature of the avalanche photodiode's impulse-response function and 2) the presence of intersymbol interference (ISI). At ultrafast transmission rates, ISI becomes a dominant component of the BER, and its effect on the BER should be carefully addressed. One solution to this problem, termed the bit-pattern-dependent (PD) approach, is to first calculate the conditional BER given a specific bit pattern and then average over all possible bit patterns. Alternatively, a simplifying method, termed the bit-pattern-independent (PI) approach, has been commonly used whereby the average bit stream is used to calculate the distribution of the receiver output, which, in turn, is used to calculate the BER. However, when ISI is dominant, the PI approximation is inaccurate. Here, the two approaches are analytically compared by analyzing their asymptotic behavior and their bounds. Conditions are found to determine when the PI method overestimates the BER. The BER found using the PD method exponentially decays with the received optical power, whereas for the PI approach, the BER converges to a constant, which is unrealistic. For an InP-based APD receiver with a 100-nm multiplication layer, the PI method is found to be inaccurate for transmission rates beyond 20 Gb/s.

Index Terms: Bit error rate (BER), optical receivers, Gaussian distribution, photodetectors, intersymbol interference (ISI), analytical models, approximation error.

1. Introduction

Avalanche photodiodes (APDs) are commonly used photodetectors in many high-speed optical receivers due to their internal optoelectronic gain, which allows the photogenerated current to dominate the thermal noise without the need for optical pre-amplification of the received optical signal. The physical phenomenon behind the internal current gain is the electron-hole impact ionization process,

which takes place in the high-field (intrinsic) multiplication layer of the APD [1]. However, the enhancement from the gain is accompanied by excess in the shot noise by a factor known as the excess noise factor, which is a measure of uncertainty associated with the stochastic nature of the APD's gain. Moreover, the APD's buildup time, which is the stochastic time required for the cascade of impact ionizations to complete per incident photon, further limits the receiver performance by causing intersymbol interference (ISI). While separate absorption and multiplication InP APDs have been successfully deployed in 10 Gb/s lightwave systems, they cannot sustain higher bit rates due to their long avalanche buildup time. Much of the recent work on APDs has focused on developing new structures and incorporating alternative materials that will yield lower noise and higher speed. For example, in 2009, a Ge/Si APD was demonstrated to have a gain-bandwidth product of 340 GHz and a sensitivity of -28 dBm [2] at 10 Gb/s. Moving toward higher transmission speed, a new approach has been proposed in [3], [4] that employs periodic bit-synchronized dynamic biasing of the APD to reduce ISI by quenching the avalanche buildup time near the end of each optical pulse. The analytical calculation of the bit-error rate (BER) of digital optical receivers that employ APDs is especially challenging due to the presence of ISI and the stochastic nature of avalanche gain and its correlation with the stochastic avalanche buildup time.

Numerous methods have been developed to approximate the BER. In [5], a procedure was given to numerically compute system performance, which uses the nearly exact Webb's approximation of the true Conradi distribution for the APD output. The measured performance of the system was found to be in excellent agreement with the performance predicted. In their model, the ISI was not addressed due to the low transmission speed. However, as it is the case in modern lightwave systems, the transmission rates are large (upwards of 10 Gb/s) and the ISI cannot be neglected. Sun *et al.* [6] developed a method to compute the exact BER based on the moment-generating function (MGF). The effects of ISI as well as the APD's dead space are both included in the analysis. The exact BER was computed by adding the contribution of every photon absorbed by the APD during every bit interval to the receiver output. However, this exact method is computationally expensive and provides no closed-form expression for the BER.

In many cases, a closed-form expression for the BER is required to understand, predict and provide analytical insight for the receiver performance. A closed-form expression for the BER can be found by first conditioning on the past bit pattern; then the BER is calculated by averaging the conditional BER over all possible past bit patterns. This approach, denoted here by the bit-pattern-dependent (PD) approach, was adopted by Ong *et al.* [7], [8] in which the receiver output, conditional on the present and all the past bits, is approximated by a Gaussian random variable. The validity of this approximation has been verified for large number of incident photons [9]. The Gaussian approximation has been shown to be quite accurate in estimating the bit error probabilities [10]. On the other hand, to simplify the analysis, another method has been commonly used by conditioning on the current bit while considering the *average* of all possible bit patterns (in place of the individual realizations of bit patterns) to generate the Gaussian distribution of the output [11]–[13]. Hence, the receiver output in this approach is bit-pattern-independent (PI), as it depends only on the average past bit pattern. However, the benefit from the simplification comes at the expense of inaccuracy in the BER when ISI is dominant, i.e., when transmission speed is very high as in the OC-192 standard.

This paper analyzes the closed-form expressions of the BER found using the PI and PD methods and studies their accuracy. To do so, the asymptotic behavior and the analytical bounds of each method are derived. By comparing the results to the numerical computed BER [6], it is found that at high transmission speeds, the PD method can give a much more accurate approximation of the BER than that offered by the PI method. This inaccuracy is negligible for low-speed applications (e.g., at 10 Gb/s) in which the ISI does not have a significant impact on the current bit. It is important to realize that even at such relatively low speed, the ISI still exists and by completely neglecting it, the BER will be underestimated. Therefore, from the asymptotic behavior, we find a photocount threshold that can be used as a decision rule to determine which approach should be used. When the photocount is below the threshold, the PI method can be adopted as a simplified approach. However, after

exceeding the photocount threshold, ISI should be properly addressed by conditioning on the entire bit pattern stream as done by the PD approach.

2. Review of Relevant BER Models

Consider a typical non-return-to-zero, on-off keying optical communication system incorporating an APD-based integrate-and-dump receiver. When an information bit 1 is transmitted, an optical pulse is transmitted in a time interval of duration T_b ; otherwise, no pulse is transmitted. Let B_n denote the input binary sequence representing the binary information in the n th bit ($n = 0$ represents current bit). Let Γ denote the raw output resulting from the integrate-and-dump receiver (i.e., prior to any decision). The information (0 or 1) can be detected by comparing Γ to a threshold, θ . Each information bit B_n contributes a term $R_n B_n$ to the receiver output, where R_n is the random variable representing the stochastic receiver output when the n th past bit is a 1 and all other past bits are 0. Thus, the receiver outputs conditioned on the current bit ($B_0 = 0$ or 1), denoted by Γ_0 and Γ_1 , respectively, can be expressed as

$$\begin{aligned}\Gamma_0 &= \sum_{n=1}^{\infty} R_n B_n + N \\ \Gamma_1 &= \sum_{n=1}^{\infty} R_n B_n + R_0 + N\end{aligned}\quad (1)$$

where N is the receiver Johnson noise. Note that only the term R_0 conveys information from the current bit. The components R_n , $n \geq 1$, represent the ISI contributions in the receiver output from the earlier bits. Due to the analytical complexity of the exact statistics of R_n , it is customary to model R_n as a Gaussian random variable.

For its relevance to the present paper, we begin by briefly reviewing the probabilistic model for the conditional receiver outputs, Γ_0 and Γ_1 , developed using the PI and PD methods to determine their BERs; these BERs are termed BER_I and BER_D . Both the mean and variance of R_n , denoted by μ_n and σ_n^2 , respectively, are shown in [7] to be proportional to the average number of photons per bit, n_0 . Additionally, they are both exponentially decreasing with the bit order n . More precisely [7],

$$\mu_0 = n_0 \beta_\mu \quad (2)$$

$$\mu_n = n_0 e^{-\kappa \lambda n} \alpha_\mu \quad (n = 1, 2, \dots) \quad (3)$$

$$\sigma_0^2 = n_0 \beta_\sigma \quad (4)$$

$$\sigma_n^2 = n_0 e^{-\kappa \lambda n} \alpha_\sigma \quad (n = 1, 2, \dots). \quad (5)$$

The coefficients α_μ , α_σ , β_μ , and β_σ are APD-specific system parameters derived in [7] as

$$\beta_\mu = \frac{\langle G \rangle}{\kappa \lambda} (\kappa \lambda - 1 + e^{-\kappa \lambda}) \quad (6)$$

$$\beta_\sigma = \frac{\langle G \rangle^2 F}{\kappa \lambda} (\kappa \lambda - 2 + 2e^{-\kappa \lambda} + \kappa \lambda e^{-\kappa \lambda}) \quad (7)$$

$$\alpha_\mu = \frac{2\langle G \rangle}{\kappa \lambda} (\cosh(\kappa \lambda) - 1) \quad (8)$$

$$\alpha_\sigma = \frac{\langle G \rangle^2 F}{\kappa \lambda} (e^{-\kappa \lambda} - 1)(1 - \kappa \lambda e^{-\kappa \lambda} - e^{-\kappa \lambda}) \quad (9)$$

where brackets represent ensemble average and F is the APD's excess noise factor, defined as $F = \langle G^2 \rangle / \langle G \rangle^2$. Sun *et al.* [11] defined the so-called shot-noise-equivalent-bandwidth as $B_{sneq} = \langle G^2 / T \rangle / 2 \langle G \rangle^2 F$, the bandwidth correlation factor as $\kappa = 4B_{sneq} / 2\pi B_{3dB}$ and the detector's relative speed as $\lambda = 2\pi B_{3dB} T_b$. The ensemble average quantities can be computed using the joint probability

density function (PDF) associated with the random variables comprising the APD's stochastic gain, G , and its stochastic avalanche duration time, T , developed in [11].

The PI method used in [11] approximates the conditional receiver outputs, Γ_0 and Γ_1 , by Gaussian random variables. In particular, BER_I is computed as [11]

$$\text{BER}_I = \frac{1}{2} \operatorname{erfc} \left(\frac{\mu_{I1} - \mu_{I0}}{\sqrt{2(\sigma_{I0} + \sigma_{I1})}} \right) \quad (10)$$

where μ_{I0} and σ_{I0}^2 denote the mean and variance of the receiver output conditional on the present bit being 0 while assuming the average of all possible patterns, i.e., $B_n = 1/2$ for $n \geq 1$. Moreover, μ_{I1} and σ_{I1}^2 are similar quantities conditional on the present bit being 1. The expressions for the parameters μ_{I0} , σ_{I0}^2 , μ_{I1} , and σ_{I1}^2 are [11]

$$\mu_{I0} = \frac{1}{2} \frac{e^{-\kappa\lambda}}{1 - e^{-\kappa\lambda}} n_0 \alpha_\mu \quad (11)$$

$$\mu_{I1} = \mu_{I0} + \beta_\mu n_0 \quad (12)$$

$$\sigma_{I0}^2 = \frac{1}{4} \sum_{n=1}^{\infty} (2\sigma_n^2 + \mu_n^2) + \sigma_N^2 \quad (13)$$

$$\sigma_{I1}^2 = \sigma_{I0}^2 + n_0 \beta_\sigma. \quad (14)$$

The optimal decision threshold, θ that minimizes BER_I is [1]

$$\theta = \frac{\mu_{I1}\sigma_{I0} + \mu_{I0}\sigma_{I1}}{\sigma_{I1} + \sigma_{I0}}. \quad (15)$$

Note that in the PI method, the distribution of the conditional receiver output has a unimodal distribution.

We next describe the PD method. Instead of assuming a Gaussian PDF for the receiver output conditional on the present bit, Ong *et al.* [7] assume a Gaussian PDF for the receiver output conditional on the present and *the entire past bit stream*. This will lead to a multimodal distribution for the conditional receiver output.

More precisely, for an arbitrary past bit pattern, $l_j \in \{0, 1\}^\infty$, the pattern-dependent means and variances of Γ_0 and Γ_1 are given by [7]

$$\mu_{D|0}(l_j) = \sum_{k=1}^{\infty} a_k(l_j) \mu_k \quad (16)$$

$$\mu_{D|1}(l_j) = \mu_{D|0}(l_j) + \mu_0 \quad (17)$$

$$\sigma_{D|0}^2(l_j) = \sum_{k=1}^{\infty} a_k(l_j) \sigma_k^2 + \sigma_N^2 \quad (18)$$

$$\sigma_{D|1}^2(l_j) = \sigma_{D|0}^2(l_j) + \sigma_0^2 \quad (19)$$

where $a_k(l_j) = 0$ unless the k th bit in the pattern l_j is a 1 bit, in which case $a_k(l_j)$ assumes the value 1. To calculate BER_D , Ong *et al.* compute the ensemble average of the pattern-specific BER over all possible past bit patterns: [7]

$$\text{BER}_D = \lim_{L \rightarrow \infty} \frac{1}{2^L} \sum_{j=1}^{2^L} \frac{1}{4} \left[\operatorname{erfc} \left(\frac{\theta - \mu_{D|0}(l_j)}{\sqrt{2}\sigma_{D|0}(l_j)} \right) + \operatorname{erfc} \left(\frac{\mu_{D|1}(l_j) - \theta}{\sqrt{2}\sigma_{D|1}(l_j)} \right) \right] \quad (20)$$

where θ is calculated for convenience from (15). Note that the optimal threshold, denoted by θ_o , does not have a simple analytical expression in this case because the PDF of the receiver output is a multimodal distribution. However, one can calculate θ_o numerically by finding the intersection point of the conditional PDFs of the receiver output. In the calculations considered in Section 4, we evaluate

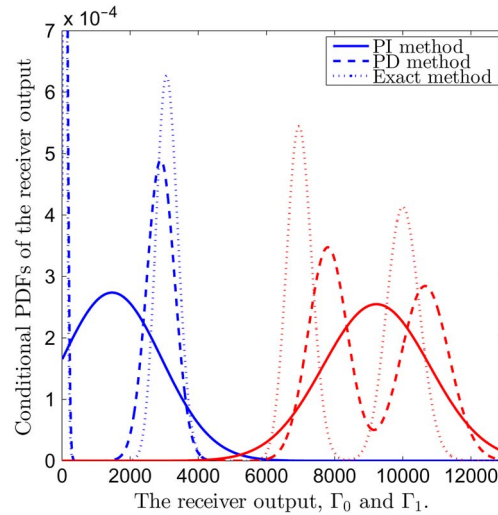


Fig. 1. PDF of an InP APD receiver output conditioned on the current bit being either 0 (blue curves) or 1 (red curves) for the PI and PD approaches. The exact conditional PDF is also shown for comparison. The average number of photons in a one transmitted bit is $n_0 = 1000$, $1/T_b = 60$ Gb/s and $L = 5$.

$BER_{D,opt}$ using the optimal threshold, θ_o , and compare it to BER_D , which uses the threshold θ . Note that we have implicitly neglected the additional current generated from the background light and tunneling. Nonetheless, the above models can be easily generalized to accommodate the dark current and the background light rates. These effects will only shift the means and increase the variances of the receiver output by adding additional interference and noise. Therefore, ignoring these effects will not influence the conclusions of this paper.

Fig. 1 shows an example of the conditional PDFs calculated for an InP-based APD with 100-nm multiplication layer. An electric field of 10.5 kV/cm was assumed in the multiplication layer, corresponding to an average gain of 10.3 and a buildup-time-limited 3-dB bandwidth of 29 GHz. The bit transmission rate is set to 60 Gb/s. The PDFs of Γ_0 and Γ_1 for the PI and PD approaches are compared to the exact PDFs found in [6]. For a linear-mode operation of the APD, the avalanche buildup time terminates at some finite random time almost surely. Therefore, in the PD approach, we can justify setting an adequate value for L to be sufficiently large to capture all the ISI terms. In our calculation, we found $L = 5$ as an appropriate value beyond which no significant change in the BER was observed. Fig. 1 foretells that the PD method yields a better approximation of the exact PDF compared to the PI approach. Also, it is clear from the figure that BER_D (as well as the exact BER) outperforms BER_I since the PDFs of the PI method are larger than that for the PD (and the exact) method in the vicinity of the decision threshold, θ .

3. Asymptotic Analysis of the BER

We now compare BER_I and BER_D for large n_0 and for various transmission rates, $1/T_b$.

3.1.1. Theorem 1

$\lim_{n_0 \rightarrow \infty} BER_I$ is a constant whereas BER_D decays exponentially in n_0 . Moreover, when n_0 exceeds the threshold

$$n_{th} \equiv -\frac{1}{c_2^2} \ln \left[\sqrt{\pi} \operatorname{erfc} \left(\frac{\beta_\mu \sqrt{1 - e^{-2\kappa\lambda}}}{\sqrt{2} e^{-\kappa\lambda} \alpha_\mu} \right) \right] \quad (21)$$

where c_2 is defined in (26), then $BER_I - BER_D > r(n_0)$, where $r(n_0)$ is a monotonically increasing positive function converging to $\lim_{n_0 \rightarrow \infty} BER_I$.

Before proving this theorem, it is worthwhile to mention that the photon count threshold, n_{th} , is a function of the bit transmission speed, $1/T_b$, reflected in the detector's relative speed factor, $\lambda = 2\pi B_{3dB} T_b$.

3.1.1.1. Proof

Consider the case for which the current bit is 0; in this case and for large n_0 ,

$$\sigma_{I|0}^2 \sim \frac{1}{4} \frac{e^{-2\kappa\lambda}}{1 - e^{-2\kappa\lambda}} \alpha_\mu^2 n_0^2. \quad (22)$$

Similarly, for the case when the current bit is 1, it can be shown that $\sigma_{I|1}^2 \sim \sigma_{I|0}^2$ when n_0 is large. Substituting these results in the error probability found in (10), we obtain

$$\lim_{n_0 \rightarrow \infty} \text{BER}_I = \frac{1}{2} \text{erfc} \left(\frac{\beta_\mu \sqrt{1 - e^{-2\kappa\lambda}}}{\sqrt{2} e^{-\kappa\lambda} \alpha_\mu} \right). \quad (23)$$

Thus, BER_I is asymptotically independent of n_0 and it saturates to a predetermined constant.

Next, we find the upper bound, $U(n_0)$, for BER_D and describe its asymptotic behavior. This is done by considering the worst (maximum error) bit-pattern scenario. Consider the first term in (20), which represents the probability of falsely announcing 1 when the current bit is 0. This term is maximized when all the past bits are 1. Similarly, the second term in (20), which represents the probability of falsely announcing 0 when the current bit is 1, is maximized when all the past bits are 0. By replacing these worst-case scenarios in (20), we obtain the following upper bound for BER_D :

$$\text{BER}_D < \frac{1}{4} \left[\text{erfc} \left(\frac{\theta - \sum_{n=1}^{\infty} \mu_n}{\sqrt{2 \sum_{n=1}^{\infty} \sigma_n^2}} \right) + \text{erfc} \left(\frac{\mu_0 - \theta}{\sqrt{2 \sum_{n=0}^{\infty} \sigma_n^2}} \right) \right]. \quad (24)$$

Using the upper bound $\text{erfc}(x) < (2/\sqrt{\pi})(e^{-x^2}/x + \sqrt{x^2 + (4/\pi)})$ [14], we further obtain

$$\text{BER}_D < \frac{1}{4\sqrt{\pi}} \left(\frac{e^{-c_1^2 n_0}}{c_1 \sqrt{n_0}} + \frac{e^{-c_2^2 n_0}}{c_2 \sqrt{n_0}} \right) \equiv U(n_0) \quad (25)$$

where c_1 and c_2 are defined as

$$c_1 = \frac{\frac{1}{2}\beta_\mu - \frac{e^{-\kappa\lambda}}{2(1-e^{-\kappa\lambda})}\alpha_\mu}{\sqrt{2 \frac{e^{-\kappa\lambda}}{1-e^{-\kappa\lambda}}\alpha_\sigma}} \quad \text{and} \quad c_2 = \frac{\frac{1}{2}\beta_\mu - \frac{e^{-\kappa\lambda}}{2(1-e^{-\kappa\lambda})}\alpha_\mu}{\sqrt{2(\beta_\sigma + \frac{e^{-\kappa\lambda}}{1-e^{-\kappa\lambda}}\alpha_\sigma)}}. \quad (26)$$

Similarly, to find a lower bound for BER_D , we consider the best (minimum error) past-bit scenarios (a past-bit stream of all 0s when considering the probability of falsely announcing 1 and a past-bit stream of all 1s when considering the probability of falsely announcing 0). By using these best-case scenarios in conjunction with the lower bound $\text{erfc}(x) > (2/\sqrt{\pi})(e^{-x^2}/(x + \sqrt{x^2 + 2}))$ [4], it can be shown that

$$\text{BER}_D > \frac{1}{4\sqrt{\pi}} \frac{e^{-c_0^2 n_0}}{c_0 \sqrt{n_0}} \quad (27)$$

where $c_0 = \beta_\mu/2\sqrt{2\beta_\sigma}$. Therefore, unlike BER_I , BER_D decays exponentially with respect to the average photon count n_0 since its upper and lower bounds decay exponentially in n_0 .

Next, consider the intersection point between $\lim_{n_0 \rightarrow \infty} \text{BER}_I$ and $U(n_0)$, which can be approximated for large n_0 by n_{th} defined in (21). Note that when $n_0 > n_{th}$, $\text{BER}_I > \text{BER}_D$; furthermore, $\text{BER}_I - \text{BER}_D > r(n_0)$ where $r(n_0) = \lim_{n_0 \rightarrow \infty} \text{BER}_I - U(n_0)$. Clearly, $r(n_0)$ is a monotonically increasing function in n_0 with $\lim_{n_0 \rightarrow \infty} r(n_0) = \lim_{n_0 \rightarrow \infty} \text{BER}_I$. ■

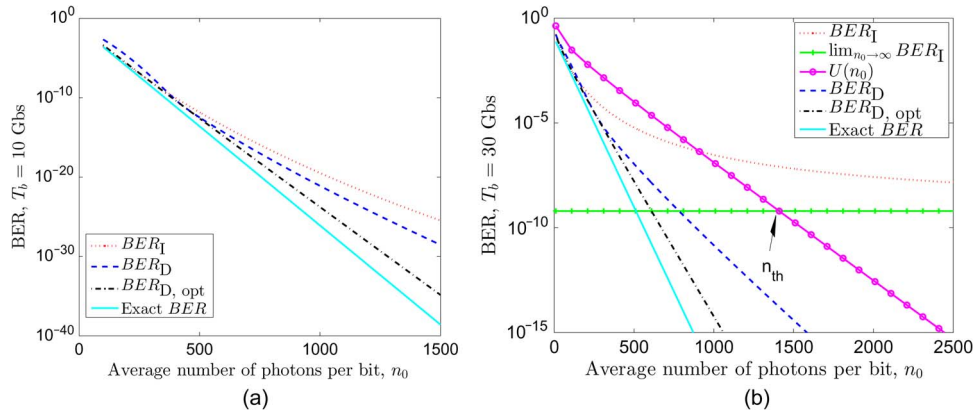


Fig. 2. The BER of an InP-based optical receiver using the two approximation methods compared to the exact BER. In the PD method, the optimal threshold, θ_o , was considered in addition to the suboptimal threshold, θ ($L = 5$). (a) BER at a transmission rate of 10 Gb/s. (b) BER at a transmission rate of 30 Gb/s.

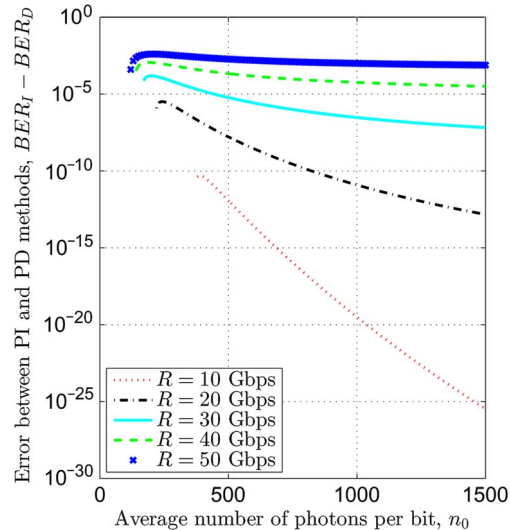


Fig. 3. The discrepancy, $BER_I - BER_D$, between the PI and PD approximation methods for different transmission rates ($L = 5$).

4. Numerical Results

In our calculations, we selected an InP-based APD receiver with a 100-nm multiplication layer and an electric field of 10.5 kV/cm. The system parameters, calculated numerically using the renewal theory approach [11], are $\alpha_\mu = 97.49$, $\alpha_\sigma = 5.5 \times 10^3$, $\beta_\mu = 7.76$, and $\beta_\sigma = 325.4$. The bit-length parameter is set to $L = 5$, which is large enough to capture all significant ISI terms for this example. The behavior of BER_I , BER_D , and $BER_{D,opt}$, are shown in Fig. 2 for two transmission rates, 10 GHz and 30 GHz. We compare the results to the exact BER calculated using the MGF approach [6]. The numerical results suggest that at low transmission rate (10 Gb/s), the PI method gives a good estimate of the BER and it can be used instead of the PD method to reduce the computational complexity. However, at 30 Gb/s, ISI becomes crucial to the BER and the PI method deviates from the exact BER and saturates at high optical powers as the asymptotic analysis predicted. On the

other hand, for the PD method, both BER_D and $BER_{D,opt}$ decay exponentially and follow the exact BER with a small difference. This difference is due to the Gaussian approximation of the actual PDFs, which are, unlike the normal distribution, asymmetric about the mean value. Therefore, we conclude that the PD method offers a better approximation to the exact BER than the PI method at high transmission rates.

The asymptotic analysis found in Section III is included in Fig. 2(b). At 10 Gb/s the photon count threshold was found from (21) to be large enough ($n_{th} \approx 10^4$) that the advantage of the PD method over the PI method are not realizable for any reasonable value of n_0 . However, by increasing the transmission speed to 30 Gbps, n_{th} drops dramatically to 1500 photons per bit, as shown in Fig. 2(b). Clearly at such speed the PI method is invalid and the PD method must be used. Fig. 3 illustrates $BER_I - BER_D$ at different transmission speeds. It is observed that the discrepancy between BER_I and BER_D widens with the transmission rate. At lower transmission rates such as 10 Gb/s, where ISI is not severe, the PI and PD methods are almost equivalent. However, at higher transmission rates, e.g., $R = 30$ Gb/s, $BER_I - BER_D = 2.9 \times 10^{-7}$ when $n_0 = 1000$, and $BER_I - BER_D = 6.6 \times 10^{-8}$ when $n_0 = 1500$.

5. Conclusion

This paper provides a rigorous comparison of two commonly used BER approximations for APD-based optical receivers. The analysis has been supported with examples and compared to the numerical BER found using the MGF approach. When ISI is dominant, the PI method overestimates the BER substantially and the PD method should be used instead. The BER of the PD method decreases exponentially with the optical energy in each bit while the BER computed using the simplified PI method saturates to a constant as the optical energy per bit increases. A closed-form expression was found for a threshold value, n_{th} , for the average number of photons per 1 bit beyond which the PD method should be used instead of the PI method. As an example, the numerical calculations show that the BER of an optical receiver utilizing InP APD with a 100 nm multiplication layer, cannot be approximated with the PI method when the system speed exceeds 20 Gb/s.

References

- [1] G. P. Agrawal, *Fiber-Optic Communication Systems*, 3rd ed. New York, NY, USA: Wiley, 2002.
- [2] Y. Kang, H.-D. Liu, M. Morse, M. J. Paniccia, M. Zadka, S. Litski, G. Sarid, A. Pauchard, Y.-H. Kuo, H.-W. Chen, W. S. Zaoui, J. E. Bowers, A. Beling, D. C. McIntosh, X. Zheng, and J. C. Campbell, "Monolithic germanium/silicon avalanche photodiodes with 340 GHz gain-bandwidth product," *Nature Photon.*, vol. 3, pp. 59–63, Jan. 2009.
- [3] M. M. Hayat and D. A. Ramirez, "Multiplication theory for dynamically biased avalanche photodiodes: New limits for gain bandwidth product," *Opt. Exp.*, vol. 20, no. 7, pp. 8024–8040, Mar. 2012.
- [4] G. El-Howayek and M. M. Hayat, "Method for performance analysis and optimization of APD optical receivers operating under dynamic reverse bias," in *Proc. IEEE IPC*, Bellevue, WA, USA, Sep. 2013, pp. 362–363.
- [5] F. Davidson and X. Sun, "Gaussian approximation versus nearly exact performance analysis of optical communication systems with PPM signaling and APD receivers," *IEEE Trans. Commun.*, vol. 36, no. 11, pp. 1185–1192, Nov. 1988.
- [6] P. Sun, M. M. Hayat, and A. K. Das, "Bit error rates for ultrafast APD based optical receivers: Exact and large deviation based asymptotic approaches," *IEEE Trans. Commun.*, vol. 57, no. 9, pp. 2763–2770, Sep. 2009.
- [7] D. S. G. Ong, J. S. Ng, M. M. Hayat, P. Sun, and J. P. R. David, "Optimization of InP APDs for high-speed lightwave systems," *J. Lightw. Technol.*, vol. 27, no. 15, pp. 3294–3302, Aug. 2009.
- [8] D. S. G. Ong, M. M. Hayat, J. P. R. David, and J. S. Ng, "Sensitivity of high-speed lightwave system receivers using InAlAs avalanche photodiodes," *IEEE Photon. Technol. Lett.*, vol. 23, no. 4, pp. 233–235, Feb. 2011.
- [9] A. Papoulis, "High density shot noise and Gaussianity," *J. Appl. Probability*, vol. 8, no. 1, pp. 118–127, Mar. 1971.
- [10] S. D. Personick, P. Balaban, J. Bobsin, and P. Kumar, "A detailed comparison of four approaches to the calculation of the sensitivity of optical fiber system receivers," *IEEE Trans. Commun.*, vol. 25, no. 5, pp. 541–548, May 1977.
- [11] P. Sun, M. M. Hayat, B. E. A. Saleh, and M. C. Teich, "Statistical correlation of gain and buildup time in APDs and its effects on receiver performance," *J. Lightw. Technol.*, vol. 24, no. 2, pp. 755–768, Feb. 2006.
- [12] J. B. Abshire, "Performance of OOK and low-order PPM modulations in optical communications when using APD-based receivers," *IEEE Trans. Commun.*, vol. 32, no. 10, pp. 1140–1143, Oct. 1984.
- [13] H. M. H. Shalaby, "Effect of thermal noise and APD noise on the performance of OPPM-CDMA receivers," *J. Lightw. Technol.*, vol. 18, no. 7, pp. 905–914, Jul. 2000.
- [14] L. C. Andrews, *Special Functions of Mathematics for Engineers*, 2nd ed., Bellingham, WA, USA: SPIE, 1992.